



Special Feature: Materials Analysis Using Quantum Beams

Research Report

Ion Diffusion in Li Battery Materials Probed by Quasi-elastic Neutron Scattering

Hiroshi Nozaki

Report received on Jun. 2, 2015

■ABSTRACT■ The diffusive characteristics of Li-ion battery materials were investigated using quasi-elastic neutron scattering (QENS) measurements. It was found that QENS is able to detect relatively rapid ionic motions even in magnetic compounds. A QENS assessment of LiMn_2O_4 , serving as a positive electrode, demonstrated a self-diffusion coefficient of approximately 10^{-8} cm^2/s . Based on the variations with temperature of the QENS spectra of the garnet-type oxides $\text{Li}_{5+x}\text{La}_3\text{Zr}_x\text{Nb}_{2-x}\text{O}_{12}$ (LLZO, $x = 0-2$), the activation energy (E_a) associated with Li diffusion is estimated to be in the range of 15 to 20 kJ/mol, and is essentially independent of x . The QENS data were in good agreement with the values of E_a obtained from $\mu^+\text{SR}$ measurements, although both E_a values were about one half of the E_a determined for the ionic conductivity of Li^+ (σ_{Li}) by assessing the AC-impedance values of sintered pellets. This result indicates the significant effects of grain boundaries and/or surfaces on E_a . This work demonstrates that QENS measurements are able to detect fast, microscopic ionic motions without any effects due to the presence of magnetic ions.

■KEYWORDS■ Quasi-elastic Neutron Scattering, Lithium, Secondary Battery, Positive Electrode, Solid Electrolyte, Ion Diffusion

1. Introduction

Since ion diffusion in batteries and fuel cells is the basic principle by which these devices function, it is necessary to understand the diffusion mechanism in order to develop novel electrode and electrolyte materials. Currently, it is important to be able to detect Li^+ diffusion in such materials, because Li-ion batteries (LIB) are seen as key components of hybrid vehicles (HV), electronic vehicles (EV) and fuel cell vehicles (FCV). In addition to electrochemical measurements that can provide the chemical diffusion coefficient (D_{chem}), there are three main techniques used to determine the self-diffusion coefficient (D) of Li^+ in solids: nuclear magnetic resonance (NMR), positive muon-spin relaxation ($\mu^+\text{SR}$) and quasi-elastic neutron scattering (QENS). NMR is the most common technique used to measure both D_{Li} and D_{H} .⁽¹⁾ However, quantitative analysis by NMR is challenging in the case of materials containing magnetic ions, due to the effect of electron spins on the spin-lattice relaxation rate. In addition, the deconvolution of the multiple components of diffusive motions is difficult because NMR detects only the average values of diffusion

motions. In such cases, we have demonstrated that it is possible to analyze the diffusive behavior of Li ions by $\mu^+\text{SR}$ measurements.⁽²⁻⁴⁾ Although it is possible to measure the Li diffusive behavior using this technique, even in magnetic materials, the upper limit of D values that may be assessed is approximately 10^{-8} to 10^{-9} cm^2/s . Thus, this method is not able to detect fast ionic motions. Herein, we propose that quasi-elastic neutron scattering (QENS) is a powerful technique for the detection of fast ionic motions in ionic-conducting materials. Since QENS is insensitive to motion below 1-10 eV (approximately 10^8 to 10^9 Hz), it is a complementary technique to $\mu^+\text{SR}$. The intensity of the QENS signal is proportional to the incoherent scattering cross section (σ_{inc}) of the target atom, thus the QENS signal from hydrogen is strong and easily detectable because the σ_{inc} of hydrogen is 80 barn ($= 80 \times 10^{-24}$ cm^2),⁽⁵⁾ representing the largest value of any element. For this reason, many QENS studies of hydrogenated materials have been reported. In contrast, the σ_{inc} of Li is 0.92 barn, which is two orders of magnitude smaller than that of H. For this reason, it takes a long time to obtain a meaningful QENS signal from Li using older-generation neutron sources.

Recently, however, accelerator-based spallation neutron sources have become operational both in Japan and in the United States, at J-PARC⁽⁶⁾ and SNS.⁽⁷⁾ Furthermore, an even more powerful neutron facility, the European Spallation Source (ESS), is being built in Lund, Sweden, close to the synchrotron radiation facility MAX-lab, with anticipated completion in 2020.⁽⁸⁾ Since such facilities provide very intense neutron beams, we expect that QENS studies of various elements, including Li, will become more common. We ourselves have performed QENS analyses of positive electrode materials and solid electrolytes intended for Li-ion batteries to show that the QENS technique is effective at detecting Li⁺ diffusive behavior.

2. Experimental

2.1 Sample Preparation

Powdered samples of ⁷LiMn₂O₄ and ⁷Li_{1.1}Mn_{1.9}O₄ (LMO) were prepared from LiOH·H₂O and MnOOH by a two-step solid state reaction. As previously reported,⁽⁹⁻¹¹⁾ well-crystallized LiMn₂O₄ compounds are available by this technique. Mixtures were subsequently made using various molar ratios of ⁷LiOH·H₂O (99.9% purity, Cambridge Isotope Laboratories, Inc., U.K.) to MnOOH (99.9% purity, Tosoh Co., Japan), and these were ground and pressed into pellets. These pellets were subsequently heated at 1000°C for 12 hours in air, crushed into powder, and repressed into pellets. The pellets were then oxidized for 24 hours in air, applying a temperature of 700°C for LiMn₂O₄ and 600°C for Li_{1.1}Mn_{1.9}O₄. Powder X-ray diffraction (XRD) measurements showed that the two samples were composed of single phases with a cubic structure having a space group of *Fd* $\bar{3}$ *m*. The magnetic susceptibility results obtained for these materials were identical to those obtained in our previous work.^(9,12) In the case of Li_{3+x}La₃Zr_xNb_{2-x}O₁₂ (LLZO, *x* = 0-2), which is employed as a solid electrolyte, powder samples in which *x* = 0, 1.75 and 2.0 were prepared by a solid-state reaction technique described in the literature.^(13,14) All samples were confirmed to have a single cubic phase with a space group of *Ia* $\bar{3}$ *d* by XRD measurements. To reduce the substantial absorption of neutrons by ⁶Li nuclei, present at a concentration of 10% in natural lithium, a ⁷Li-enriched source was used for the preparation of both LMO and LLZO. This treatment

was remarkably effective in terms of improving the neutron scattering measurements, especially when working at longer wavelengths.

2.2 QENS Experiments

Two different spectrometers were used for QENS analyses of LMO: a disk chopper spectrometer (DCS)⁽¹⁵⁾ and a high flux backscattering spectrometer (HFBS),⁽¹⁶⁾ both located at NIST Center for Neutron Research (NCNR) in the United States. For DCS measurements, we employed a neutron wavelength of 6.5 Å, while a wavelength of 6.27 Å was used for HFBS studies. The energy resolutions during DCS and HFBS analyses were approximately 50 and 1 μeV. The temperature, *T*, range over which measurements were performed was 5-550 K in the case of the DCS and 80-500 K for the HFBS. The powder samples were held in a cylindrical vanadium container filled with He gas for DCS measurements and in a double walled cylindrical aluminum container filled with air for HFBS measurements. QENS spectra of LLZO were obtained on the backscattering BASIS spectrometer⁽¹⁷⁾ situated at Spallation Neutron Source (SNS) at Oak Ridge National Laboratory, over the *T* range of 150 to 600 K. The μ⁺SR and QENS signal intensities are proportional to the volume fraction of the target material. Since the particle size of the polycrystalline samples was approximately 10 μm, almost the entire QENS signal originated from the sample bulk rather than the grain boundary or the surface. The neutron data were packed, analyzed and visualized using the DAVE software package.⁽¹⁸⁾

2.3 QENS Analysis

The measured neutron scattering intensity, *I*(*Q*, ω), represents a convolution of the incoherent scattering function *S*_{inc}(*Q*, ω) and the resolution function, *R*(*Q*, ω), as follows:

$$I(Q, \omega) = \int_{-\infty}^{\infty} S_{\text{inc}}(Q, \omega) R(Q, \omega - \omega') d\omega', \quad (1)$$

where *Q* and ω are the momentum and the energy transfer, respectively. Because the QENS signal is usually observed together with the elastic neutron scattering signal that defines the instrumental resolution, the spectra are fitted by a combination of a delta function, $\delta(\omega)$, derived from the instrumental

resolution, and a Lorentzian function, as in following equation:

$$S_{\text{inc}}(Q_0, \omega') = A(Q_0) \delta(\omega') + \frac{1}{\pi} \frac{\Gamma_{Q_0}}{\Gamma_{Q_0}^2 + \hbar^2 (\omega' - \omega_0)^2}, \quad (2)$$

in which $A(Q_0)$ is the intensity of the δ function, Γ_{Q_0} is the width of the Lorentzian and \hbar is the Planck's constant.

The normalized mean-square displacement (MSD) $\delta \langle u^2 \rangle = \langle u^2 \rangle(T) - \langle u^2 \rangle(T \rightarrow 0 \text{ K})$,⁽¹⁸⁾ which is obtained from the elastic neutron scattering intensity as follows:

$$\delta \langle u^2 \rangle = \int_{-\infty}^{\infty} F S_{\text{inc}}(Q, \omega = 0) u^2 du, \quad (3)$$

where F and u are the spatial Fourier transform operator and the displacement, respectively.

3. Results

3.1 LiMn₂O₄

Figure 1(a) shows the T dependence of the MSD values of ${}^7\text{LiMn}_2\text{O}_4$ and ${}^7\text{Li}_{1.1}\text{Mn}_{1.9}\text{O}_4$. For both samples, $\delta \langle u^2 \rangle$ increases as T increases from 90 K to approximately 360 K, although the slope, $d\delta \langle u^2 \rangle/dT$, suddenly increases in the vicinity of 280 K. Above 360 K, the $\delta \langle u^2 \rangle$ of ${}^7\text{Li}_{1.1}\text{Mn}_{1.9}\text{O}_4$ plateaus at a constant value up to 460 K, while the $\delta \langle u^2 \rangle$ of ${}^7\text{LiMn}_2\text{O}_4$ continues to slowly increase up to 460 K. The anomaly at approximately 280 K indicates that the lattice vibrations deviate from the Debye approximation above 280 K, the natural result of changes in the diffusion of Li and/or Mn ions with variations in σ_{inc} . In contrast, since the σ_{inc} of oxygen is negligibly small (0.0008 barn) compared with those of Mn (0.4 barn) and ${}^7\text{Li}$ (0.78 barn),⁽¹⁹⁾ neither the shift in the oxygen position nor changes in the oxygen deficiency contribute to the change in the slope at 280 K. This result indicates that Li ions begin to diffuse above 280 K, because the spinel framework would not be stable at room temperature if the Mn ions were to diffuse above 280 K. Similar diffusive behavior has also been reported based on $\mu^+\text{SR}$ measurements.⁽²⁰⁾ Figure 1(b) shows the energy spectra obtained for both ${}^7\text{LiMn}_2\text{O}_4$ and ${}^7\text{Li}_{1.1}\text{Mn}_{1.9}\text{O}_4$ at 400 K, in which a QENS signal is clearly observed together with an elastic signal that defines the instrumental resolution.

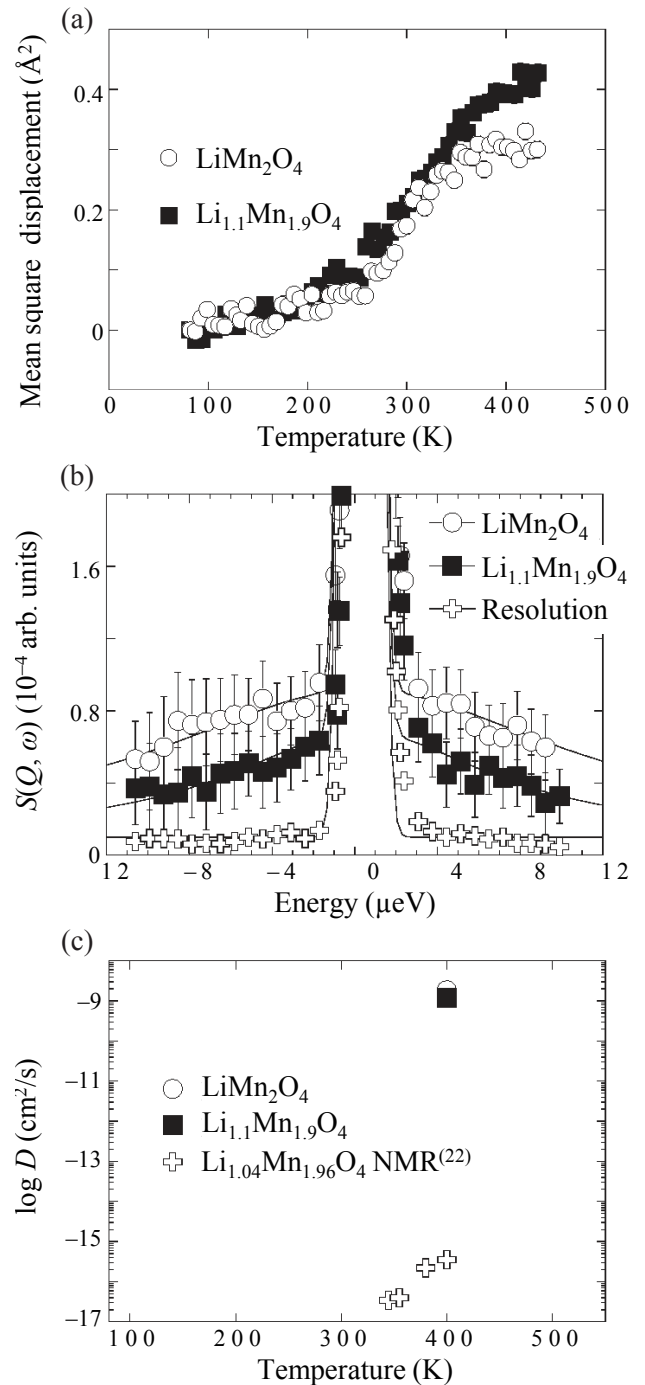


Fig. 1 (a) T dependence of the mean-square displacement for LiMn_2O_4 and $\text{Li}_{1.1}\text{Mn}_{1.9}\text{O}_4$. (b) The Q integrated energy spectra of LiMn_2O_4 and $\text{Li}_{1.1}\text{Mn}_{1.9}\text{O}_4$ at 400 K. The full width at half maximum (FWHM) values of the two samples are estimated to be 12.0(0) and 7.7(1) μeV , respectively. To improve the statistics, the energy increments were rebinned from the original data. The spectra comprise data for the integrated intensities over the Q range between 0.25 and 1.75 \AA^{-1} . (c) A comparison of the diffusion coefficients obtained from the present neutron studies and from the previously reported NMR data in Ref. (22), on a logarithmic scale.

The Lorentzian fit provides a full width at half maximum (FWHM; $= \Gamma_{Q_0}$) of approximately $12.0(0)\mu\text{eV}$ for ${}^7\text{LiMn}_2\text{O}_4$ and approximately $7.7(1)\mu\text{eV}$ for ${}^7\text{Li}_{1.1}\text{Mn}_{1.9}\text{O}_4$. It should also be noted that the FWHM values obtained from QENS in the magnetic diffuse scattering range were on the order of several μeV at low temperatures and were outside of the measurable range in the case of the HFBS. Therefore, there are no magnetic contributions to the estimated values of Γ_{Q_0} . From the equation $\Gamma_{Q_0} = D_s^{\text{Li}} Q^2$, we are able to obtain $D_s^{\text{Li}} = 1.8(4) \times 10^{-8} \text{ cm}^2/\text{s}$ at 400 K for ${}^7\text{LiMn}_2\text{O}_4$, and $1.1(8) \times 10^{-8} \text{ cm}^2/\text{s}$ at 400 K for ${}^7\text{Li}_{1.1}\text{Mn}_{1.9}\text{O}_4$, assuming that Q_0 is approximately equal to 1 \AA^{-1} . This is an average Q value for the spectrometer and is typical of the values reported for the ionic diffusion lengths in solids.⁽²¹⁾ Surprisingly, the obtained D_s^{Li} is larger than the D_s^{Li} estimated for LiMn_2O_4 using Li-NMR data⁽¹⁾ by six orders of magnitude (Fig. 1(c)). It is well known that the spin-lattice relaxation rate of the NMR signal is strongly affected by magnetic ions, resulting in difficulty in correctly estimating D_s^{Li} ,⁽²⁾ and so there have been few reliable D_s^{Li} values reported for LiMn_2O_4 . According to first principles calculations of the value of D_s^{Li} for LiTi_2O_4 , D_s^{Li} should be in the vicinity of $2 \times 10^{-10} \text{ cm}^2/\text{s}$ at 300 K.⁽²²⁾ Furthermore, recent $\mu^+\text{SR}$ measurements of LiCoO_2 have demonstrated that the D_s^{Li} of $\text{Li}_{0.73}\text{CoO}_2$ is approximately $7 \times 10^{-10} \text{ cm}^2/\text{s}$ at 300 K.⁽²³⁾ Therefore, the D_s^{Li} value obtained for LiMn_2O_4 by QENS is reasonable for a Li-ion battery electrode material.

3.2 Solid Electrolyte

Interestingly, the ionic conductivity (σ_{Li}) of LLZO has been found to depend on x and to reach a maximum at $x = 1.75$ at ambient temperature, for reasons currently unknown.^(13,14) There are two potential parameters that may determine σ_{Li} : the diffusion coefficient of Li^+ (D_{Li}) and the number density of mobile Li^+ ions (n_{Li}). While it is unfortunately difficult to measure n_{Li} directly, there are three microscopic techniques by which the intrinsic D_{Li} values of solids may be determined:⁽²⁴⁻²⁶⁾ NMR, QENS and $\mu^+\text{SR}$.

Figure 2 shows the QENS spectra for the $x = 0$, 1.75 and 2.0 samples. The incoherent elastic intensity ($S_{\text{inc}}^{\text{E}}$) is seen to decrease with T and a quasi-elastic peak with a broad Lorentzian shape appears above 300 K, likely due to Li diffusion. The T -dependent incoherent quasi-elastic intensity ($S_{\text{inc}}^{\text{QE}}$) is calculated as follows:

$$S_{\text{inc}}^{\text{QE}}(T) = [S_{\text{inc}}^{\text{E}}(300 \text{ K}) - S_{\text{inc}}^{\text{E}}(T)]/S_{\text{inc}}^{\text{E}}(300 \text{ K}). \quad (4)$$

Above 300 K, $S_{\text{inc}}^{\text{QE}}(T)$ increases with T for each sample (**Fig. 3**). Note that the slope ($dS_{\text{inc}}^{\text{QE}}/dT$) for the $x = 0$ sample is roughly the same to that for the $x = 2$ sample, while the slope for the $x = 1.75$ sample is the steepest.

Assuming that the Li diffusion process in LLZO is thermally activated, we can estimate the activation energy (E_a) from the $\nu(T)$ and $S_{\text{inc}}^{\text{QE}}(T)$ curves. **Figure 4** shows the x dependence of E_a values estimated from $\mu^+\text{SR}$ ($E_a^{\mu\text{SR}}$)⁽²⁷⁾ and QENS (E_a^{QENS})⁽²⁸⁾ data, together with the values determined by AC impedance measurements (E_a^{AC}).⁽¹³⁾ It is evident that $E_a^{\mu\text{SR}}$ is comparable to E_a^{QENS} , as expected, although both values are almost one half of E_a^{AC} . A very similar discrepancy between the E_a values obtained by NMR and AC impedance measurements has been reported previously for several materials.⁽²⁴⁾ This suggests that the overall diffusion of Li^+ is not

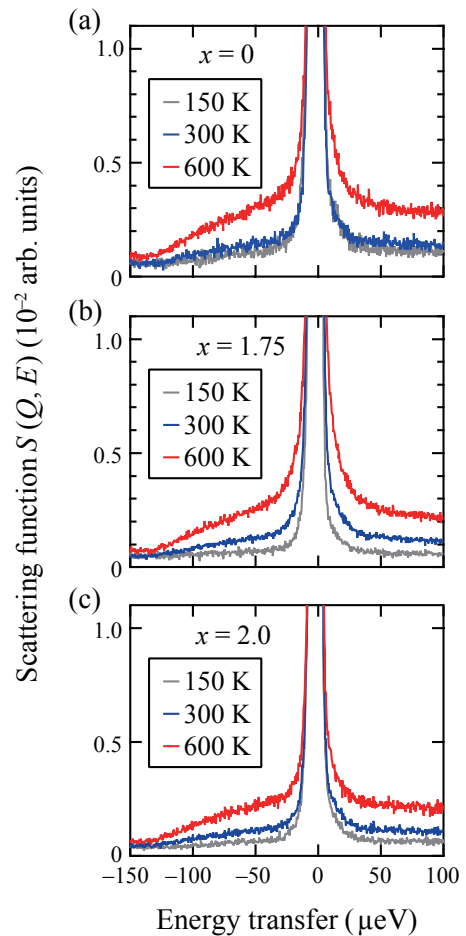


Fig. 2 T dependence of $S(Q, E)$ for the $x = 0$, 1.75 and 2.0 samples. The FWHM of each QENS spectrum appear similar to one another, suggesting that the self-diffusion coefficient is almost the same at each x .

determined by the intrinsic properties of LLZO but rather by other factors, such as grain boundaries, impurities and defects. As such, it should be possible to reduce E_a^{AC} by improving the sample preparation process.

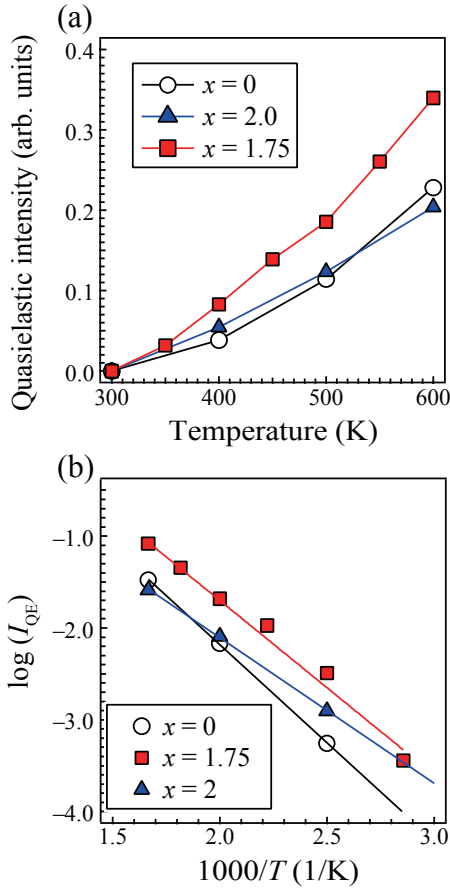


Fig. 3 (a) The T dependence of S_{inc}^{QE} and (b) S_{inc}^{QE} as a function of $1/T$.

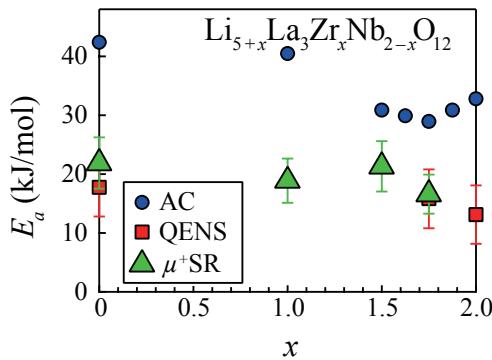


Fig. 4 Relationship between the thermal activation energy (E_a) and x for LLZONb. Triangles and squares represent E_a values estimated by μ^+ SR and QENS. Circles represent E_a values determined by AC impedance measurements.⁽¹³⁾

In the case of LLZO, it was difficult to analyze the D_{Li} due to the unfavorable statistics of the QENS data, although D_{Li} was roughly estimated to be in the range of 10^{-7} to 10^{-9} cm^2/s based on the FWHM determined from the QENS spectrum. The value of D_{Li} has also been estimated using the muon-spin relaxation (μ^+ SR) technique,⁽²⁷⁾ which has been described in detail elsewhere.⁽²⁵⁾ The D_{Li} for LLZO are shown in **Fig. 5(a)** together with the ionic conductivity (σ_{Li}). Interestingly, D_{Li} is essentially independent of x , especially at $x \geq 1$. According to the Nernst-Einstein equation (Eq. (5)), σ_{Li} is associated with both D_{Li} and the density of mobile Li^+ (n_{Li}).

$$D_{Li} = \frac{\sigma_{Li}RT}{n_{Li}F^2Z^2}, \quad (5)$$

where R is the gas constant, F is Faraday's constant and Z is the ionic valence. Since LLZO is an electronic insulator over the entire range of x used in this study, we naturally assumed that only Li^+ is responsible for charge transport in this material. Here, we may introduce a term giving the number of mobile Li^+ ions per unit cell: $C_{Li}^{eff} \{ \equiv n_{Li}/[a^3(5+x)] \}$, where a is the LLZO lattice constant. Figure 5(b) shows C_{Li}^{eff} as a function of x . The $C_{Li}^{eff}(x)$ curve has the same appearance as the σ_{Li} curve, since D_{Li} is almost constant over this x range. The $C_{Li}^{eff}(x)$ values vary by a factor of about 7.5,

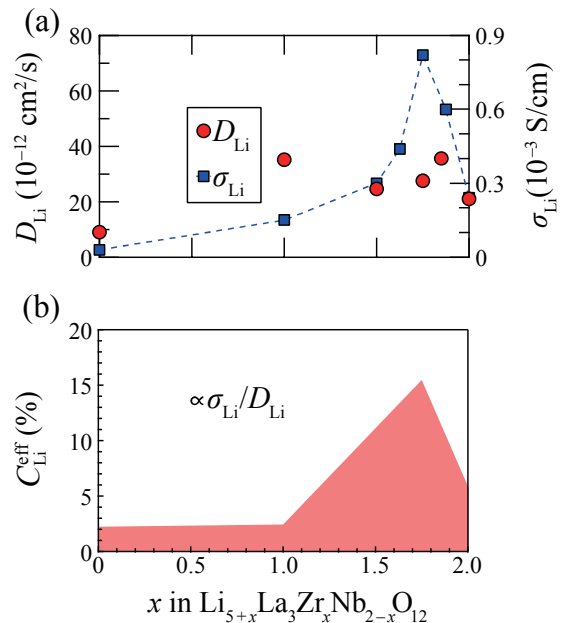


Fig. 5 x dependences of (a) D_{Li} obtained by μ^+ SR and σ_{Li} obtained from AC impedance measurements and (b) the number of mobile Li^+ per unit cell.

which is sufficiently large compared to the uncertainty in n_{Li} . Consequently, it has been demonstrated that the value of σ_{Li} is primarily determined by the number of mobile Li^+ ions rather than by the value of D_{Li} . Even in the case of LLZO with $x = 1.75$, which exhibits the highest σ_{Li} value, the proportion of mobile Li^+ out of all the Li in the lattice is only 15%. The origin of the mobile Li^+ ions is still unknown, and it will be necessary to clarify the relationship between $C_{\text{Li}}^{\text{eff}}$ and x using other techniques, such as QENS and NMR, to resolve this question.

4. Conclusion

We performed QENS measurements of Li-ion battery materials as a means of investigating their ionic conducting behavior. In the case of the LiMn_2O_4 spinel, we were able to assess the diffusion characteristics of Li^+ above 280 K for both LiMn_2O_4 and $\text{Li}_{1.1}\text{Mn}_{1.9}\text{O}_4$, and the self-diffusion coefficient was estimated to be approximately 10^{-8} cm²/s at 400 K for both compounds. For the Li-garnet compounds (LLZO), intended for use as solid electrolytes, the Li^+ diffusion activation energy was almost independent of Li content. Based on a combined analysis with $\mu^+\text{SR}$, it was found that the ionic conductivity in LLZO is governed by the number of mobile Li^+ . The QENS signals for the Li compounds are not easy to detect because the incoherent cross section (σ_{inc}) of Li is two orders of magnitude lower than that of the hydrogen atom. However, the advent of high neutron flux facilities such as J-PARC, SNS and ESS has made it possible to obtain QENS measurements of lithium, and we have succeeded in detecting the diffusive behavior of Li^+ using QENS. Therefore, QENS should be applied not only to the study of anode, cathode and solid electrolyte materials intended for Li-ion batteries, but also to the analysis of a wider variety of ion-conducting materials composed of other ions, such as Na^+ , K^+ and I^- .

Acknowledgements

The authors wish to thank the staff of NIST, SNS and J-PARC for assistance with the neutron scattering experiments.

References

- (1) Verhoeven, V. W. J., de Schepper, I. M., Nachtegaal, G., Kentgens, A. P. M., Kelder, E. M., Schoonman, J. and Mulder, F. M., *Phys. Rev. Lett.*, Vol. 86, No. 19 (2001), pp. 4314-4317.
- (2) Sugiyama, J., Mukai, K., Ikedo, Y., Nozaki, H., Månsson, M. and Watanabe, I., *Phys. Rev. Lett.*, Vol. 103, No. 14 (2009), 147601.
- (3) Sugiyama, J., Ikedo, Y., Mukai, K., Nozaki, H., Månsson, M., Ofer, O., Harada, M., Kamazawa, K., Miyake, Y., Brewer, J. H., Ansaldo, E. J., Chow, K. H., Watanabe, I. and Ohzuku, T., *Phys. Rev. B*, Vol. 82, No. 22 (2010), 224412.
- (4) Sugiyama, J., Nozaki, H., Harada, M., Kamazawa, K., Ofer, O., Månsson, M., Brewer, J. H., Ansaldo, E. J., Chow, K. H., Ikedo, Y., Miyake, Y., Ohishi, K., Watanabe, I., Kobayashi, G. and Kanno, R., *Phys. Rev. B*, Vol. 84, No. 5 (2011), 054430.
- (5) Sears, V. F., *Neutron News*, Vol. 3, No. 3 (1992), pp. 29-37.
- (6) J-PARC (Japan Proton Accelerator Research Complex), <<http://j-parc.jp/index.html>>, (accessed 2015-06-01).
- (7) ORNL Neutron Sciences, <<http://neutrons.ornl.gov/>>, (accessed 2015-06-01).
- (8) ESS(European Spallation Source), <<http://europenspallationsource.se/>>, (accessed 2015-06-01).
- (9) Sugiyama, J., Mukai, K., Ikedo, Y., Russo, P. L., Suzuki, T., Watanabe, I., Brewer, J. H., Ansaldo, E. J., Chow, K. H., Ariyoshi, K. and Ohzuku, T., *Phys. Rev. B*, Vol. 75, No. 17 (2007), 174424.
- (10) Kitagawa, M., Wakabayashi, H., Ariyoshi, K. and Ohzuku, T., *ITE Lett. on Batteries, New Technol. & Medicine*, Vol. 8 (2007), p. 119.
- (11) Mukai, K., Sugiyama, J., Ikedo, Y., Nozaki, H., Kamazawa, K., Andreica, D., Amato, A., Månsson, M., Brewer, J. H., Ansaldo, E. J. and Chow, K. H., *Z.J. Phys. Chem. C*, Vol. 114 (2010), No. 25, pp. 11320-11327.
- (12) Sugiyama, J., Mukai, K., Ikedo, Y., Russo, P. L., Suzuki, T., Watanabe, I., Brewer, J. H., Ansaldo, E. J., Chow, K. H., Ariyoshi, K. and Ohzuku, T., *J. Mater. Sci.: Materials in Electronics*, Vol. 19, No. 8-9 (2008), pp. 875-882.
- (13) Ohta, S., Kobayashi, T. and Asaoka, T., *J. Power Sources*, Vol. 196, No. 6 (2011), pp. 3342-3345.
- (14) Ohta, S., Kobayashi, T., Seki, J. and Asaoka, T., *J. Power Sources*, Vol. 202 (2012), pp. 332-335.
- (15) Copley, J. R. D. and Cook, J. C., *Chem. Phys.*, Vol. 292, No. 2-3 (2003), pp. 477-485.
- (16) Meyer, A., Dimeo, R. M., Gehring, P. M. and Neumann, D. A., *Rev. Sci. Instrum.*, Vol. 74, No. 5 (2003), pp. 2759-2777.
- (17) Mamontov, E. and Herwig, K. W., *Review of Scientific Instruments*, Vol. 82, No. 8 (2011), 085109.
- (18) Azuah, R. T., Kneller, L. R., Qiu, Y., Tregenna-Piggott, P. L. W., Brown, C. M., Copley, J. R. D.

- and Dimeo, R. M., *J. Res. Natl. Inst. Stand. Technol.*, Vol. 114, No. 6 (2009), pp. 341-358.
- (19) Chudley, C. T. and Elliot, R. J., *Proc. Phys. Soc.*, Vol. 77, No. 2 (1961), pp. 353-361.
- (20) Kaiser, C. T., Verhoeven, V. W. J., Gubbens, P. C. M., Mulder, F. M., de Schepper, I., Yaouanc, A., de Réotier, P. D., Cottrell, S. P., Kelder, E. M. and Schoonman, J., *Phys. Rev. B*, Vol. 62, No. 14 (2000), pp. R9236-R9239.
- (21) Hempelmann, R., *Quasielastic Neutron Scattering and Solid State Diffusion* (2000), 316p., Clarendon Press Oxford.
- (22) Bhattacharya, J. and der Ven, A. V., *Phys. Rev. B*, Vol. 81, No. 10 (2010), 104304.
- (23) Sugiyama, J., Atsumi, T., Hioki, T., Noda, S. and Kamegashira, N., *J. Alloys Compd.*, Vol. 235, No. 2 (1996), pp. 163-169.
- (24) Heitjans, P. and Indris, S., *J. Phys.: Condens. Matter*, Vol. 15, No. 30 (2003), pp. R1257-R1289.
- (25) Sugiyama, J., Mukai, K., Ikedo, Y., Nozaki, H., Månsson, M. and Watanabe, I., *Phy. Rev. Lett.* Vol. 103, No. 14 (2009), 147601.
- (26) Sugiyama, J., *J. Phys. Soc. Jpn.* Vol. 82 (2013), SA023.
- (27) Nozaki, H., Harada, M., Ohta, S., Watanabe, I., Miyake, Y., Ikedo, Y., Jalarvo, N. H., Mamontov, E. and Sugiyama, J., *Solid State Ionics*, Vol. 262 (2014), pp.585-588.
- (28) Nozaki, H., Harada, M., Ohta, S., Jalarvo, N. H., Mamontov, E., Watanabe, I., Miyake, Y., Ikedo, Y. and Sugiyama, J., *J. Phys. Soc. Jpn.* Vol. 82 (2013), SA004.

Fig. 1

Reprinted from *Phys. Rev. B*, Vol. 83 (2011), 094401, Kamazawa, K. et al., Interrelationship between Li^+ Diffusion, Charge, and Magnetism in ${}^7\text{LiMn}_2\text{O}_4$ and ${}^7\text{Li}_{1.1}\text{Mn}_{1.9}\text{O}_4$ Spinel: Elastic, Inelastic, and Quasielastic Neutron Scattering, © 2011 APS, with permission from American Physical Society.

Fig. 2

Reprinted from *J. Phys. Soc. Jpn.* Vol. 82 (2013), SA004, Nozaki, H. et al., Diffusive Behavior of Li Ions in Garnet $\text{Li}_{5+x}\text{La}_3\text{Zr}_x\text{Nb}_{2-x}\text{O}_{12}$ ($x = 0-2$), © 2013 JPSJ, with permission from The Physical Society of Japan.

Figs. 3-5

Reprinted from *Solid State Ionics*, Vol. 262 (2014), pp. 585-588, Nozaki, H. et al., Li Diffusive Behavior of Garnet-type Oxides Studied by Muon-spin Relaxation and QENS, © 2014 Elsevier, with permission from Elsevier.

Hiroshi Nozaki

Research Fields:

- Materials Science Using X-rays, Neutrons and Muons

Academic Degree: Dr.Eng.

Academic Societies:

- The Physical Society of Japan
- The Japan Institute of Metals and Materials
- The Japanese Society for Synchrotron Radiation Research
- The Japanese Society for Neutron Science
- Society of Muon and Meson Science of Japan

Awards:

- Best Poster Award of International Conference on Neutron Scattering, 2013
- Hamon President Choice, The Japan Society for Neutron Science, 2014

